Connectome Pathways in Parkinson's Disease Patients with Deep Brain Stimulators

Connectome Pathways in Parkinson's Disease Patients with DBS

Giorgio Bonmassar and Nikos Makris
AA. Martinos Center for Biomedical Imaging, MGH, Harvard Medical School,
Boston, USA.
e-mails: gbonmassar@partners.org and nmakris@partners.org

Abstract— The overarching goal of this paper is to optimally control the implanted programmable generator (IPG), a critical device that delivers electrical currents or potentials to treat neurological symptoms in patients with Parkinson' Disease (PD). Current IPG programming is based on trial and error empirical assessment, which makes the treatment implementation cumbersome, long, frustrating and expensive for the patient. Furthermore, the manifestation of the effects of IPG programming in some patient populations (e.g., dystonia) can be apparent after days, weeks or even months, which makes the trial and error approach unmanageable. Thus, the optimal IPG programming is critical to alleviate the patient's neurological symptoms. Their programming relies on parameter definition, such as electrode pair, amplitude and frequency. The positioning of the electrodes in a specific anatomical target region of interest (ROI), such as STN is limited by the surgical procedure and presurgical planning. Knowledge of the morphometry of the target ROI and its topographic relationships with surrounding anatomical structures such as whiter matter fibers (such as the internal capsule and the H1 and H2 fields of Forel) and other gray matter structures (such as the zona incerta, the substantia nigra and the red nucleus) allows the precise positioning of the stimulating electrode pair. We show that connectome imaging technology provides the necessary detailed and comprehensive in-vivo imaging of white matter fiber architecture. Based on our previous DBS studies, we present a novel numerical head model to develop a novel IPG programmer to assist neurologist in the patient management.

Keywords-deep brain brain stimulation; DBS; Parkinson's Disease; PD; MRI; DTI; implanted programmable generator; IPG; programming; connectome; STN

I. INTRODUCTION

More than 100,000 Parkinson' Disease (PD) patients worldwide have been treated with Deep Brain Stimulation (DBS) during the last twenty years resulting in 25–75% improvement of movement disorder symptoms of PD. The outcome of DBS neurosurgery depends principally on the precision of the implanted electrode placement and the ability to find the optimum settings for the Implantable Pulse Generator (IPG), a critical device for post-operative clinical management [1]-[3]. Although the theoretical basis of DBS for PD targets, such as the subthalamic nucleus (STN) and the internal part of globus pallidus (GPi) has been studied extensively in the 1980s and early 1990s, the exact mechanism of how electrical stimulation affects brain cells is not known with certainty. Given that in PD loss of dopaminergic cells leads to excessive activity in the STN and GPi, it is thought that IPGs correct this abnormal activity by injecting high-frequency electrical pulses. With respect to neurosurgery per se, DBS involves minimal permanent brain changes, however, there can be side effects, which are variable. *Most common side effects with STN implants are ataxic gait and tonic muscle contractions, paresthesias and diplopia, as well as behavioral manifestations such as depression, mania and impulse dysregulation. These are thought to be related mainly to (a) misplacement of the implanted electrodes, (b) local deformation of tissue and tissue scaring due to surgery, and (c) suboptimal programming of the IPG.* Currently, there is no realistic DBS model for IPG programming taken from actual patients with DBS implant as proposed herein. The state-of-the-art numerical DBS modeling is based on a wire or set of wires, which represents the virtual DBS implant, superimposed to healthy human brains [1, 2] (IARIA). Such models are incomplete since they do not take in consideration an accurate anatomical modeling of the fine-grained composition of the anatomic structures and their surrounding architecture involved in the stimulation, anisotropic dielectric constants and the tissue scar from the surgery. Therefore, for an enhanced VPS model and IPG programming we need detailed knowledge about the i) structural and functional anatomy of the targets and surrounding tissue, ii) encapsulating tissue around the electrode and iii) conductivity and permittivity along x, y, z, s. Post-surgical management may last several years after surgery and can be difficult. Easily adjustable or programmable IPGs (with no need of further surgery) are extremely helpful and, probably the most important tools for the neurologist to manage the PD patient long term. Therefore, safe and successful use of DBS relies heavily upon our capability to program (or adjust) the IPG. Usually, in most patients there is a reduction in levodopa medication after DBS surgery of the STN. If IPG programing is optimal, besides minimizing side effects and a safer use of DBS in PD, it can reduce or discontinue pharmacological treatment in post-surgical patients with PD. However, optimal IPG programming needs detailed knowledge of anatomical structure and function of the brain circuitry involved. Thus it seems plausible that developing and testing new IPGs optimized by Virtual Patient Stimulator (VPS) models, which are informed by precise anatomical and physiological data in

 ISBN: 978-1-61208-390-2

the individual patient will improve the therapeutic effects of neurostimulation on brain circuitry and the brain structures affected in PD. In section II we introduce: (A) the MRI acquisition methods used, (B) the numerical electromagnetic simulations performed. In section III we outlined the tractography and electromagnetic fields estimated by our simulations as well as the predicted neuronal firing frequency. In section IV we discussed our results and presented the conclusion of our study.

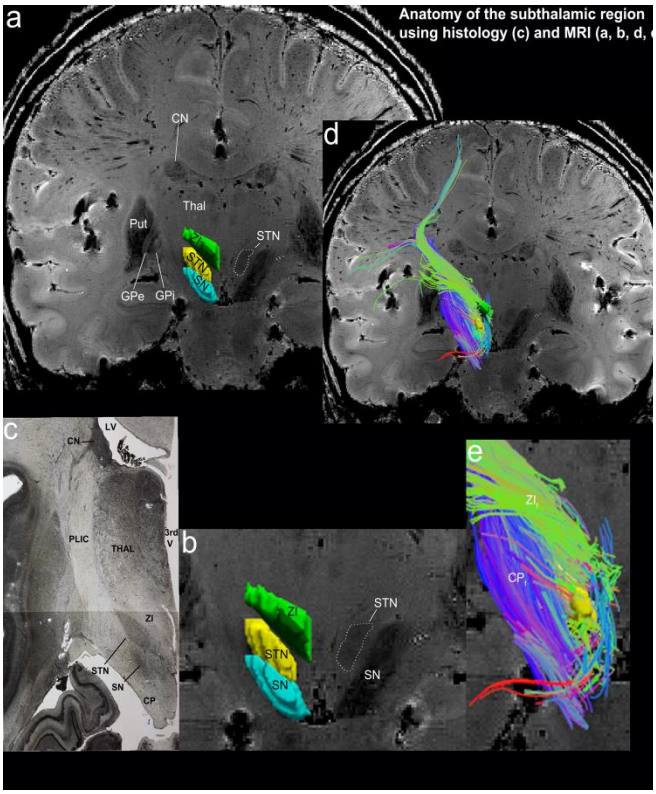

Figure 1. Anatomy of the subthalamic region using histology (c) and MRI (a, b, d, e).

II. METHODS

A. Overview of study design

The study is based on *ex-vivo* analysis of collected 7 Tesla (7T) T2* and Connectome diffusion MRI data.

(a) *Structural T2* 7 Tesla MRI* This *ex-vivo* brain consisted of MRI data of a hemisphere fixed in Periodate-Lysine-Paraformaldehyde (PLP) using the following parameters: T2*-W, 100 μm^3 isotropic resolution, TR/TE/flip=40ms/20ms/20°, 1600×1100×896 matrix. *(b)* *Connectome DSI data* are transformed into DTI data to estimate complex relative permittivity tensor $\hat{\varepsilon}^* = \frac{\varepsilon^*}{d} \cdot \mathbf{D}$, where ε* is the tissue complex relative permittivity **D** is the DTI tensor and *d* is the diffusivity. The vmPFC-BG tract is delineated using diffusion Connectome data as shown in Figure 1(b). DTI/DSI data are visually validated by comparing the computed fiber tracks with anatomical atlases with particular emphasis to the basal ganglia region. Finally, DTI/DSI data provide detailed information on the fiber tract connectivity between the STN and other parenchymal areas that is useful for DBS programming [3] and basic neuroscience research. The diffusion data set was collected on the MGH Connectome scanner with a diffusion weighted spin echo EPI sequence (1.5^3 mm^3 resolution, 140^2 matrix, FoV 210 mm, 95 slices, 128 diffusion directions at 5000 s/mm^2 and 10 b=0 acquisitions, TR 8.8 s, TE 57 ms, 3x GRAPPA acceleration, 64 channel head array) and the T1-weighted anatomical was collected on the MGH 7 T scanner with a 3D FLASH (0.4^3 mm^3 resolution, 512^2 matrix, FoV 205 mm, 352 slices, FA 30°, TR 35 ms, TE 10.2 ms, 32 channel head array).

One dataset was obtained from the Human Connectome Project (Washington Univ-Minnesota), with high spatial resolution of 1.25 mm (isotropic) (highest b-value of 3000 s/mm^2), on T1-weighted anatomical images. The *Washington U-Minnesota datasets* diffusion dataset was collected with a diffusion weighted spin echo EPI sequence (1.25^3 mm^3 resolution, 168^2 matrix, FoV 210 mm, 111 slices, 89/90/91 diffusion directions at each of 1000 s/mm^2, 2000 s/mm^2 and 3000 s/mm^2 collected with LR and RL phase encoding and 6 b=0 acquisitions, FA 78°/160°, TR 5.52 s, TE 89.5 ms, 6/8 partial Fourier, 3x multiband acceleration, 1488 Hz/px, 32 channel head array) and the T1-weighted anatomical was collected with a 3D MPRAGE (0.7^3 mm^3 resolution, 320^2 matrix, FoV 224 mm, 256 slices, FA 8° non-selective water excitation, TR 2.4 s, TE 2.14 ms, TI 1 s, asymmetric echo, 2x GRAPPA acceleration, 210 Hz/px, 32 channel head array).

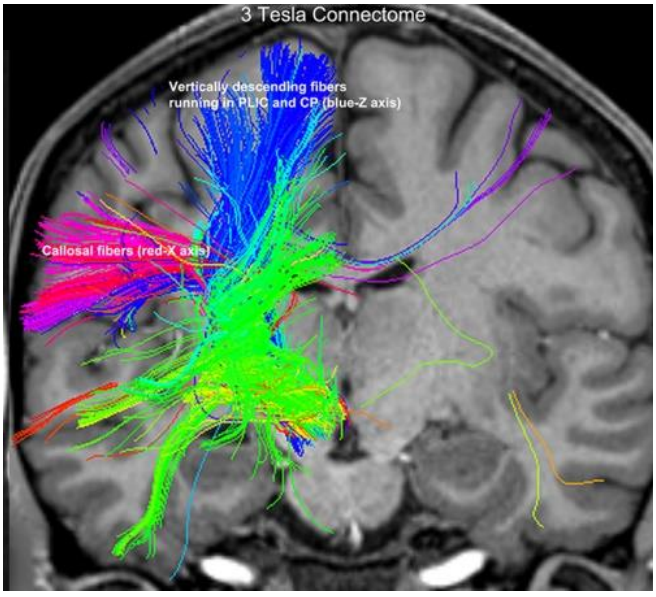

Figure 2. Diffusion imaging tractographic results in the 3 Tesla Washington U-Minnesota datasets.

B. Numerical Model of Deep Brain Stimulation implant

One or two bilateral implants, as shown by the post-operative MRI, are modeled as insulated wire(s) connected to the left and/or right targets in the head [4]. The wires are modeled as a Perfect Electrical Conductor and the dielectric is modeled as Teflon. A four-electrode connection [3] and the scar tissue are modeled in full detail reaping the benefits of the proposed 100 μm^3 isotropic resolution based on the actual Medtronic electrode set that will be used. The four electrodes are modeled as PEC and the scar tissue is modeled with the known dielectric properties.

III. RESULTS

In the following, we present preliminary results for structural imaging.

Figure 1 shows diffusion tractography results on a T1 anatomical image. We performed whole brain tractography using our state-of-the art tractography algorithm [5] capable of handling multiple fiber crossings. Subsequently, tracts connecting the STN and other brain regions were extracted. As seen in Figure 2, shows a zoomed-in portion of the tracts connecting the STN, including the ansa lentricularis fibers (green) and the other fiber bundles (blue, red). Thus, high spatial resolution, as in the connectome data, is critical for accurate tracing of these tracts, which can lead to a better understanding of the neural fiber bundles connecting STN and other sub-cortical regions around the STN. Note that, a slight misplacement of the electrode could result in the excitation of a completely different neural network, resulting in unwanted side effects. Figure 3.A shows the spatial distribution of electric field amplitude overlaid with the precise anatomy of the area surrounding the DBS implant. The field produced for the narrow bipolar stimulation configuration 1-2 is shown for three different encapsulation layer conditions. There were no differences in electric field calculated at the baseline (no encapsulation) or at the chronic stage, with a peak intensity of the electric field in both cases equal to 7.54 V/mm. Conversely, the electric field changed dramatically for the acute stage, where the higher conductivity of CSF generated a peak electric field equal to 3.59 V/mm, i.e., less than half compared to baseline or chronic stage. Furthermore, the model at the acute stage resulted in an electric field that was more spread along the electrode and asymmetric compared to the chronic stage. The electric field for the acute-stage model was characterized by higher intensity at 10mm distance from the electrode (20.33 mV/mm vs. 3.97 mV/mm). Differences in electric field between acute vs. chronic model (Figure 3.B) were also visible in the vicinity of the electrode (left), on the cortex (middle) and on the scalp (right). The stimulation was attenuated by the encapsulation, with 18% reduction in electric field amplitude delivered in the acute case and only 14% in the chronic case. The electromagnetic solution analysis was performed both in the area that surrounds the electrode and far from the electrode, i.e., on the scalp. We estimated the potential distribution for the electrode configuration 1-2 in the baseline case and compared our results with those reported in the literature. We report for the potential a drop of 84% within 4 mm of the electrode (Figure 3.C), which is in agreement with the results provided in [6]-[9] for bipolar DBS with ± 1 V voltage.

In Figure 3.D is shown the typical output of the neuron model with 117 neurons/axons, which is the status either one or zero indicates the absence or presence of an action potential. The neuron modelled was the same done by McIntyre [6], in the modeling of DBS. The electrical parameters were: conductivity=0.7/Ohm-m, membrane capacitance=0.1 uF/cm^2/lamella membrane, and membrane conductivity=0.001 S/cm^2/lamella membrane. The pulse parameters were: width = 0.1 //ms, amplitude= 3V.

IV. DISCUSSION

In order to avoid misplacements of the implanted electrodes, as well as to accurately target the sensorimotor parts of the nucleus at its dorsolateral zone [7], we need to have an accurate mapping and clear anatomical understanding of the subthalamic region. Although the allowed margin of error is 5 mm, in excellent neurosurgical procedures the error does not exceed 1 mm. However, in routine DBS practice, the margin of error is variable and several times misplacement of electrodes is such that the STN can be entirely missed. Thus the use of atlases with an estimate of the intersubject variability like the ones proposed in this study would be very useful in routine DBS neurosurgery.

Accurate tracing of the fiber connections from the STN and surrounding sub-cortical regions (e.g., substantia nigra) is critical for understanding the effect of stimulation on the neural fiber bundles connected to the STN. A small misplacement of the electrode (by a few millimeters) can result in excitation of a completely different neural circuit in the brain. Thus, accurate localization of the STN and the surrounding subcortical structures in the diffusion MRI (dMRI) images along with tractography of the associated fiber network is an essential component of our proposed work. Since the subcortical structures of interest are very small (only a few millimeters), high spatial resolution of the dMRI images is extremely important to accurately delineate these structures.

The next step will include to validate the model at a patient level. The model outlined in this abstract will be tested to check if it provides valid prediction of some or all side effects recorded in the patient and surfaced during IPG programming at different parameter settings.

V. ACKNOWLEDGMENT

National Institute of Health, National Institute of Biomedical Imaging and Bioengineering 1R21EB016449-01A1.

 ISBN: 978-1-61208-390-2

REFERENCES

[1] E. B. Montgomery, Deep brain stimulation programming : principles and practice. Oxford UK ; New York: Oxford University Press, 2010.

[2] C. C. McIntyre, S. Miocinovic, and C. R. Butson, "Computational analysis of deep brain stimulation," Expert Rev Med Devices, vol. 4, Sep 2007. pp. 615-22.

[3] C. C. McIntyre, S. Mori, D. L. Sherman, N. V. Thakor, and J. L. Vitek, "Electric field and stimulating influence generated by deep brain stimulation of the subthalamic nucleus," Clin Neurophysiol, vol. 115, Mar 2004. pp. 589-95.

[4] L. Angelone, J. Ahveninen, J. Belliveau, and G. Bonmassar, "Analysis of the Role of Lead Resistivity in Specific Absorption Rate for Deep Brain Stimulator Leads at 3 T MRI," IEEE Trans Med Imaging, Mar 22 2010. pp. 1029-38.

[5] S. A. Mohsin, N. M. Sheikh, and U. Saeed, "MRI-induced heating of deep brain stimulation leads," Phys Med Biol, vol. 53, Oct 21 2008. pp. 5745-56

[6] T. Eichele, et al. "Prediction of human errors by maladaptive changes in event-related brain networks," Proc Natl Acad Sci U S A, vol. 105, , Apr 22 2008, pp. 6173-8.

[7] J. M. Henderson, J. Tkach, M. Phillips, K. Baker, F. G. Shellock, and A. R. Rezai, "Permanent neurological deficit related to magnetic resonance imaging in a patient with implanted deep brain stimulation electrodes for Parkinson's disease: case report," Neurosurgery, vol. 57,discussion E1063, Nov 2005. p. E1063

[8] Y. Rathi, B. Gagoski, K. Setsompop, O. Michailovich, P. E. Grant, and C. F. Westin, "Diffusion propagator estimation from sparse measurements in a tractography framework," Med Image Comput Comput Assist Interv, vol. 16, 2013. pp. 510-7.

[9] N. Yousif, R. Bayford, P. G. Bain, and X. Liu, "The peri-electrode space is a significant element of the electrode-brain interface in deep brain stimulation: a computational study," Brain Res Bull, vol. 74, Oct 19 2007. pp. 361-8,

[10] S. Miocinovic, et al. , "Computational analysis of subthalamic nucleus and lenticular fasciculus activation during therapeutic deep brain stimulation," J Neurophysiol, vol. 96, Sep 2006. pp. 1569-80.

[11] A. M. Kuncel and W. M. Grill, "Selection of stimulus parameters for deep brain stimulation," Clin Neurophysiol, vol. 115, Nov 2004. pp. 2431-41.

[12] C. C. McIntyre, A. G. Richardson, and W. M. Grill, "Modeling the excitability of mammalian nerve fibers: influence of afterpotentials on the recovery cycle," J Neurophysiol, vol. 87, Feb 2002. pp. 995-1006.

[13] B. A. Strickland, J. Jimenez-Shahed, J. Jankovic, and A. Viswanathan, "Radiofrequency lesioning through deep brain stimulation electrodes: a pilot study of lesion geometry and temperature characteristics," J Clin Neurosci, vol. 20, Dec 2013. pp. 1709-12.

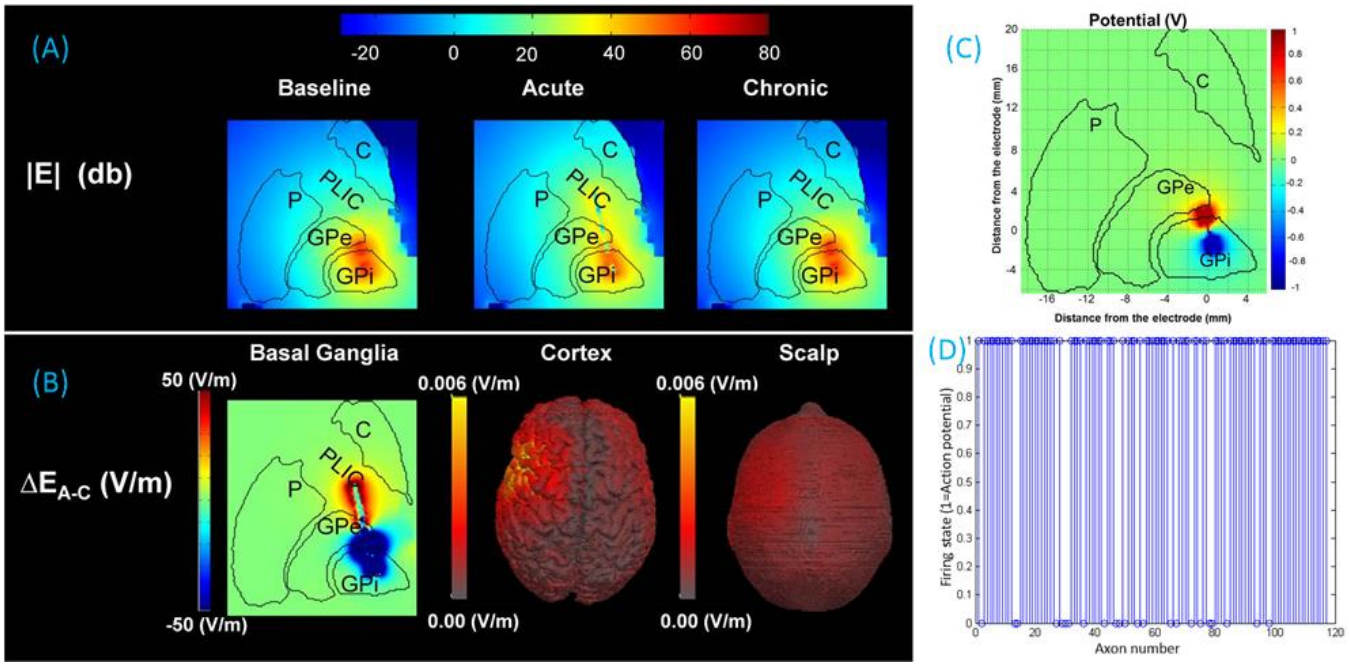

Figure 3. Electromagnetic and neural simulations. (A) Electric field |E| for: baseline (left), acute (middle), and chronic (right). (B) ΔEA-C between the acute and the chronic stage (left), on the cortex (middle row), and on the scalp (right) (C) Distribution of the potential in the vicinity of the electrode. (D) Example of firing state.

 ISBN: 978-1-61208-390-2